

miR-338-3p suppresses the malignancy of T-cell lymphoblastic lymphoma by downregulating HOXA3

LI WANG^{1*}, MINGHUA SUI^{2*} and XIULI WANG³

Departments of ¹Hematology, ²Medical Oncology and ³Gynecology,
The Affiliated Yantai Yuhuangding Hospital of Qingdao University, Yantai, Shandong 264000, P.R. China

Received August 18, 2018; Accepted May 10, 2019

DOI: 10.3892/mmr.2019.10451

Abstract. T-cell lymphoblastic lymphoma (T-LBL) is an aggressive malignancy with poor prognosis due to frequent relapses. Previous studies have reported an association of the disease with abnormal chromosomal rearrangements, DNA copy number alterations and mutations in critical signaling factors, such as those in the Notch1 pathway; however, the molecular mechanisms underlying the development of the disease remain unclear, limiting the development of novel therapies. In the present study, gene expression was detected by qPCR and western blot analysis. Diagnostic analysis was performed by ROC curve. Cell proliferation, invasion and migration were analyzed by cell proliferation and Transwell assays. Gene interactions were analyzed using luciferase reporter assay. In the present study, it was observed that the expression levels of microRNA-338-3p (miR-338-3p) were reduced in patient lymphoma tissues and a T-LBL cell line. Upregulation of its expression inhibited the migration and proliferation of cultured T-LBL cells. Bioinformatics analysis of putative target mRNAs of miR-338-3p identified a direct binding site in the 3'-untranslated of homeobox A3 (HOXA3). The levels of HOXA3 mRNA and protein were associated with those of miR-338-3p, and overexpression of HOXA3 promoted the malignant phenotype of T-LBL cells. The results suggested that miR-338-3p may suppress the development of T-LBL via the downregulation of oncogenic factors, such as HOXA3. The findings indicated that further investigation into miR-338-3p and the HOXA3 regulatory network may aid the development of novel therapeutic tools.

Introduction

Lymphoblastic lymphoma (LBL) is an aggressive neoplasm of precursor T and B cells, also known as lymphoblasts. Precursor T-cell lymphoblastic lymphoma (T-LBL) accounts for ~90% of LBL cases (1). It is predicted to derive from malignant thymocytes that may appear at defined stages of intrathymic T-cell differentiation (1). Patients are typically young males with a median age of ~20 years (2). The disease is associated with progressive infiltration of lymphoblasts into nodal structures or extranodal structures, particularly the bone marrow, spleen and central nervous system (CNS), leading to life-threatening compression of adjacent structures (3). T-LBL is a chemotherapy-sensitive disease with a 75-85% event-free survival rate using current treatment regimens (2,4); however, 5-year overall survival remains poor for T-LBL, mainly due to relapse, often as a result of spread to the CNS (2,4). Thus, suppressing the viability and invasive ability of T-LBL tumor cells may ameliorate T-LBL and improve the prognosis of patients.

There is limited information regarding cytogenetic and molecular abnormalities in T-LBL due to the rarity of the disease; it has been reported that the disease is associated with chromosomal rearrangements and submicroscopic DNA copy number alterations (5). The majority of chromosomal abnormalities involve juxtaposition of strong promoters and enhancers from T-cell receptor genes with transcriptional factor genes, including T-cell acute lymphocytic leukemia 1, lymphoblastic leukemia-derived sequence 1 and homeobox 11 (HOX11) (6). Additionally, a number of T-LBL cases have been reported to exhibit mutations in the key factors of Notch1 signaling, including those involved in ubiquitin-mediated protein degradation to regulate Notch1 protein levels, and various downstream targets that can induce cell transformation via the regulation of cell survival, proliferation and metabolism (7-11). Aberrantly upregulated Notch1 signaling has been observed in the majority of T-LBL cases, and thus Notch1 has been considered to be one of the key regulators in early T-cell development and T-LBL oncogenesis (12).

MicroRNAs (miRNAs/miRs) are endogenous small noncoding RNAs composed of 22-24 nucleotides, acting as post-transcriptional gene regulators (13,14). Aberrant expression of miRNAs can be oncogenic or tumor-suppressive, due to altered regulation of cell migration, invasion, proliferation,

Correspondence to: Dr Xiuli Wang, Department of Gynecology, The Affiliated Yantai Yuhuangding Hospital of Qingdao University, 20 Yuhuangding East Road, Zhifu, Yantai, Shandong 264000, P.R. China
E-mail: fnoejj5@163.com

*Contributed equally

Key words: T-cell lymphoblastic lymphoma, microRNA-338-3p, homeobox A3, proliferation, migration

apoptosis and chemoresistance (13,14). Recent studies have indicated the importance of miRNAs in malignant T-cell transformation (13,14). miR-338-3p is encoded in the seventh intron of the apoptosis-associated tyrosine kinase gene. Its function was first associated with prion-induced neurodegeneration, as its expression is reduced in the brains of mice infected with mouse-adapted scrapie (15). Its expression was also observed to be dysregulated in a variety of cancer types, such as lung cancer (16); however, the role of miR-338-3p in lymphoblastic lymphoma is yet to be reported.

In the present study, it was reported that the expression levels of miR-338-3p were reduced in the tissues of patients with T-LBL and in a T-LBL cell line. Its normal expression appeared to be required to inhibit the proliferation and migration of cancer cells via direct regulation of HOXA3 mRNA. The present study provided a novel insight into the molecular mechanisms underlying dysregulated signaling networks that may be involved in the pathogenesis of T-LBL.

Materials and methods

Tissue samples. T-cell lymphoblastic lymphoma (T-LBL) tissues and adjacent normal tissues were surgically isolated from 38 patients at The Affiliated Yantai Yuhuangding Hospital of Qingdao University between February 2013 and March 2015. Inclusion criteria were: i) Newly diagnosed cases; ii) no therapies performed. Exclusion criteria were: i) Recurrent cases; ii) other clinical disorders observed. Patients were staged according to Ann Arbor staging system (17). The tissues were flash-frozen in liquid nitrogen and stored at -80°C until subsequent use. The application of human samples was approved by the Human Ethics Committee/Institutional Review Board of the Affiliated Yantai Yuhuangding Hospital of Qingdao University, and all patients provided informed consent.

Cell culture and transfection. The T-LBL cell line SUP-T1, two T-cell lymphoblastic leukemia cell lines (CCRF-CEM and Jurkat) and one human T-cell line (H9) were purchased from the American Type Culture Collection. The cells were cultured in RPMI-1640 medium (Gibco; Thermo Fisher Scientific, Inc.) supplemented with 10% heat-inactivated fetal bovine serum (FBS; Thermo Fisher Scientific, Inc.). The cultured cells were incubated at 37°C with 5% CO₂.

miR-338-3p mimics, miR-338-3p inhibitor, negative control (NC) and inhibitor NC were designed and synthesized by Shanghai GenePharma Co., Ltd. Sequences were: miR-338-3p mimics, 5'-UUUGAGCAGCACUCAUUUUUGC-3'; negative control (NC), 5'-CAGUACUUUUAGUGUGUACAA-3'; miR-338-3p inhibitor, 5'-CAACAAAUCACUGAUGCUGG A-3'; inhibitor NC, 5'-UUGUAAGUUGCGACAGCCACU CA-3'. A homeobox A3 (HOXA3) plasmid for HOXA3 over-expression vector (pcDNA3.1 plasmid), and an empty vector (pcDNA3.1 plasmid) used as the NC, were purchased from Guangzhou RiboBio Co., Ltd. Nucleic acids (50 nM miRNA and 150 nM inhibitor) were mixed with Lipofectamine® 2000 (Invitrogen; Thermo Fisher Scientific, Inc.) and transfected into cells according to the manufacturer's protocol. Briefly, approximately 5-6x10⁵ SUP-T1 cells were seeded and cultured overnight to reach 90-95% confluency at the time of transfection. Nucleic acids and Lipofectamine® 2000 were diluted

in transfection medium. The reagents were then mixed and incubated at room temperature for 5 min prior to the addition of cells. The cells were further incubated at 37°C in a CO₂ incubator until subsequent assays were performed. Cells were harvested at 48 h post-transfection for subsequent experimentation.

Reverse transcription-quantitative polymerase chain reaction (RT-qPCR). Total RNA was extracted from cells or tissues using TRIzol® (Invitrogen; Thermo Fisher Scientific, Inc.), according to the manufacturer's protocol. Total RNA (1 µg) was reverse transcribed into cDNA using specific stem-loop RT primers and Mir-XTM miRNA First Strand Synthesis kit (Takara Biotechnology Co., Ltd.) or the Affinity-Script QPCR cDNA Synthesis kit (Agilent Technologies, Inc.); RT reaction was carried out at 42°C for 60 min and was terminated by heating at 70°C for 5 min. qPCR reactions were performed according to the standard SYBR Green assay protocol, and the signals were detected using an ABI PRISM 7500 Sequence Detection system (Applied Biosystems; Thermo Fisher Scientific, Inc.). qPCR was performed using a SYBR Premix Ex Taq kit (Takara Biotechnology Co., Ltd.) to determine HOXA3 expression. U6 small nuclear RNA and GAPDH were used as normalization controls for the quantification of miR-338-3p and HOXA3 expression, respectively. PCR settings were: Preheating at 95°C for 10 min, followed by 40 cycles of 95°C for 10 sec, 60°C for 20 sec, and 72°C for 10 sec. The relative expression of each gene was determined using the 2^{-ΔΔC_q} method (18). The primers used for qPCR were as follows: miR-338-3p, forward 5'-TGCGGTCCAGCATCAGTGAT-3', reverse 5'-CCAGTG CAGGGTCCGAGGT-3'; HOXA3, forward 5'-TGGCAGTTT TACTTTATTGTTCATAGC-3', reverse 5'-CATCAGAAATGT CCTGCTTGC-3'. U6, forward, 5'-GCTCGCTTCGGCAGC ACA-3'; U6, reverse, 5'-GAGGTATTTCGACCAGAGGA-3'; GAPDH, forward, 5'-ACACCCACTCCTCCACCTTT-3'; GAPDH, reverse, 5'-TTACTCCTTGGAGGCCATGT-3'.

Cell proliferation assay. Cells were transfected and seeded in 96-well plates at 2x10³ cells/well. The cells were further cultured in a 37°C, 5% CO₂ incubator for 0, 24, 48 and 72 h. Then, 10 µl of Cell Counting Kit-8 (CCK-8; Beyotime Institute of Biotechnology) reagent was added to each well. The 96-well plates were further incubated for 2 h under the aforementioned conditions. The absorbance was detected at 450 nm using a microplate reader.

Cell migration assay. Following transfection and incubation for 24 h, cells were further cultured in serum-free medium for 12 h. The cells were suspended, and the concentrations were adjusted to 4-5x10⁵ cells/ml. Transwell chambers with 8-µm pores (Corning, Inc.) were placed in 24-well plates. RPMI-1640 medium (500 µl) containing 10% FBS was added to the lower chambers, and suspended cells (200 µl) were plated in the upper chambers. The plates were further incubated for 10 h at 37°C. Cells on the lower surface of the chamber were fixed with 20% glacial acetic acid for 15-30 min and stained with 0.1% crystal violet for 30 min at 37°C. The total number of cells was estimated from 10 randomly selected fields. An inverted microscope (Nikon Corporation) was used; magnification, x400.

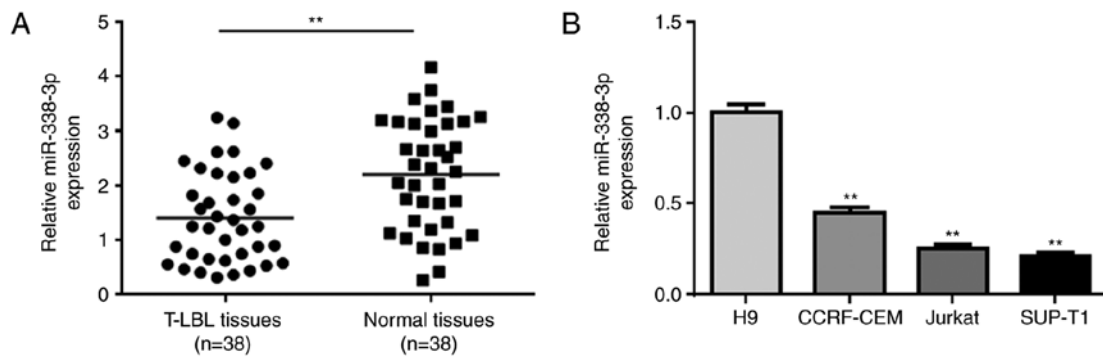


Figure 1. Reduced expression of miR-338-3p in T-LBL. (A) RT-qPCR analysis of miR-338-3p expression in 38 pairs of T-LBL tissues and adjacent normal tissues. (B) RT-qPCR analysis of miR-338-3p expression in the normal H9 cell line, the T-LBL cell line SUP-T1 and two lymphoblastic leukemia cell lines (CCRF-CEM and Jurkat). ** $P < 0.01$ vs. H9. miR-338-3p, microRNA-338-3p; RT-qPCR, reverse transcription-quantitative PCR; T-LBL, T-cell lymphoblastic lymphoma.

Luciferase reporter assay. According to predictions made using the TargetScan database (release 7.2; <http://www.targetscan.org>), a putative miR-338-3p-binding site was identified in the 3'-untranslated region (3'-UTR) of the HOXA3 gene. The HOXA3 wild-type (WT) 3'-UTR sequence and a mutant version (MT) were amplified via PCR and cloned into the pGL3 dual-luciferase reporter vector (Promega Corporation) to create pGL3-HOXA3-3'-UTR-WT (WT vector) and pGL3-HOXA3-3'-UTR-MT (MT vector). Source of the DNA was human HOXA3 cDNA; polymerase: Pyrobest DNA polymerase (Fermentas; Thermo Fisher Scientific, Inc.). The primers used were: WT, forward, 5'-CCGCTCGAGGAGCCAGGAGTC ACTAGG-3', and reverse, 5'-TAAGCGGCCGCTTGTTCAG AACGTGAG-3'. The PCR settings were 94°C for 3 min; 35 cycles at 94°C for 30 sec, 55°C for 30 sec and 72°C for 30 sec; terminated at 72°C for 5 min. SUP-T1 cells in the logarithmic growth phase were seeded into 96-well plates at 1.5×10^4 cells/well, and co-transfected with the 100 ng WT or 100 ng MT vector and one of the 50 nM miRNA or 150 nM inhibitor (miR-338-3p mimics, NC, miR-338-3p inhibitor or inhibitor NC) using Attractene Transfection Reagent (Qiagen, Inc.). Following incubation for 48 h, the ratio of firefly to *Renilla* luciferase activity was determined using a dual-luciferase reporter system, according to the manufacturer's protocols (Promega Corporation).

Western blotting. Cells were collected and lysed in ice-cold RIPA buffer (Beyotime Institute of Biotechnology) with 10 mM PMSF. Protein concentration was determined using the bicinchoninic acid (BCA) protein assay kit (Beyotime Institute of Biotechnology), and equal amounts of the samples (50 μ g per lane) were separated via 10% SDS-PAGE. Proteins were then transferred to polyvinylidene fluoride membranes at 100 V for 2.5 h. The membranes were blocked for 2 h at room temperature with 5% fat-free milk in TBS with Tween-20 and incubated with primary antibodies specific for HOXA3 (Abcam, ab28771) and GAPDH (Abcam, ab9485) at 4°C overnight. Then, HRP Goat Anti-Rabbit (IgG) secondary antibody (Abcam, ab6721; 1:5,000) were added for incubation at room temperature for 2 h. Chemiluminescence reagents were used to visualize the signals (EMD Millipore). ImageJ v1.38 software (National Institutes of Health) was used to quantify protein expression levels. GAPDH was used as the loading control.

Statistical analysis. Statistical analyses were performed using SPSS 17.0 software (SPSS, Inc.). All the experiments were performed at least three independent times. Data are presented as the mean \pm standard deviation. According to the miR-338-3p mean expression level, 38 cases of T-LBL tissues samples were divided into two groups, including a higher miR-338-3p expression group (n=20) and a lower miR-338-3p expression group (n=18). Correlations between clinicopathological characteristics and miR-338-3p expression were analyzed by χ^2 test. Independent-samples t-tests were performed to compare two independent groups. One-way ANOVA followed by Bonferroni's post-hoc test was performed to analyze differences between three or more independent groups. $P < 0.05$ was considered to indicate a statistically significant difference.

Results

Reduced expression of miR-338-3p in T-LBL. To investigate the role of miR-338-3p in T-LBL, the expression levels of miR-338-3p were measured in T-LBL and adjacent normal tissues collected from 38 patients with T-LBL. The mean expression levels of miR-338-3p were significantly decreased in T-LBL tumor tissues compared with those in the normal tissues (Fig. 1A). The expression levels were associated with certain clinicopathological characteristics (Table I). The levels of miR-338-3p were also determined in a number of cell lines, which were predicted to be more homogeneous than those in patient samples. miR-338-3p was significantly downregulated in the T-LBL cell line SUP-T1, and the lymphoblastic leukemia cell lines CCRF-CEM and Jurkat, compared with in the human H9 T-cell line (Fig. 1B).

Overexpression of miR-338-3p suppresses cell proliferation and migration. SUP-T1 cells were used for further functional analyses. Synthetic miR-338-3p and miR-338-3p inhibitor molecules were transfected into the SUP-T1 cells to rescue and further reduce miR-338-3p expression, respectively (Fig. 2A). CCK-8 assays were performed to determine the proliferation of cells at 24, 48, and 72 h post-transfection. Transfection with miR-338-3p mimics significantly decreased the proliferation of the cancer cells compared with the NC, whereas further reducing miR-338-3p expression with the inhibitor

Table I. Clinicopathological characteristics of patients with T-cell lymphoblastic lymphoma with high or low miR-338-3p expression.

Characteristic	No. of patients (n=38)	miR-338-3p expression		P-value
		Low (n=18)	High (n=20)	
Sex				0.351
Male	28	12	16	
Female	10	6	4	
Age, years				0.573
<40	29	13	16	
>40	9	5	4	
B-symptoms				0.564
Yes	13	7	6	
No	25	11	14	
BM involvement				0.184
Yes	9	6	3	
No	29	12	17	
Bulky disease (>10 cm)				0.018
Yes	22	14	8	
No	16	4	12	
Ann Arbor stage				0.021
I/IE or II/IIIE	11	2	9	
III/IV	27	16	11	
Albumin				0.351
≤35 g/dl	10	6	4	
>35 g/dl	28	12	16	
Therapy response				0.386
CR	27	14	13	
Not CR	11	4	7	
Relapse in 2 years				0.010
Yes	23	7	16	
No	15	11	4	

BM, bone marrow; CR, complete response; miR-338-3p, microRNA-338-3p.

significantly promoted SUP-T1 cell proliferation (Fig. 2B). Additionally, Transwell assays were performed to investigate cell migration. Similarly, upregulated miR-338-3p expression significantly reduced cell migration, whereas transfection with inhibitor enhanced migration compared with the respective controls (Fig. 2C). The results suggested that rescuing the expression of miR-338-3p may suppress the development of T-LBL.

miR-338-3p directly regulates HOXA3 expression by targeting its 3'-UTR. As miRNAs mainly associate with the 3'-UTR of mRNAs to regulate gene expression, searches were performed to identify putative targets of miR-338-3p to investigate the molecular mechanisms underlying its activity. TargetScan was employed to search for miR-338-3p target genes, particularly those with potential roles in promoting tumor cell proliferation and migration. HOXA3 was considered a good candidate for further analysis (Fig. 3A). The

3'-UTR of HOXA3 was introduced into a dual-luciferase reporter system, and the effects of altering miR-338-3p expression on luciferase production were investigated. Introducing miR-338-3p mimics into cells significantly suppressed luciferase signals, whereas transfection with miR-338-3p inhibitor further increased luciferase activity, compared with the respective controls. Conversely, cells transfected with a dual-luciferase vector containing a mutant 3'-UTR that did not form a duplex with the seed-pairing region of miR-338-3p did not exhibit alterations in luciferase activity following transfection with mimics or inhibitor (Fig. 3B). The levels of HOXA3 protein and mRNA in SUP-T1 cells were then further assessed. Transfection with miR-338-3p mimics significantly downregulated HOXA3 at the protein and mRNA levels compared with the NC, whereas decreasing the levels of miR-338-3p upregulated HOXA3 (Fig. 3C and D). The results indicated that miR-338-3p directly targeted the 3'-UTR of HOXA3.

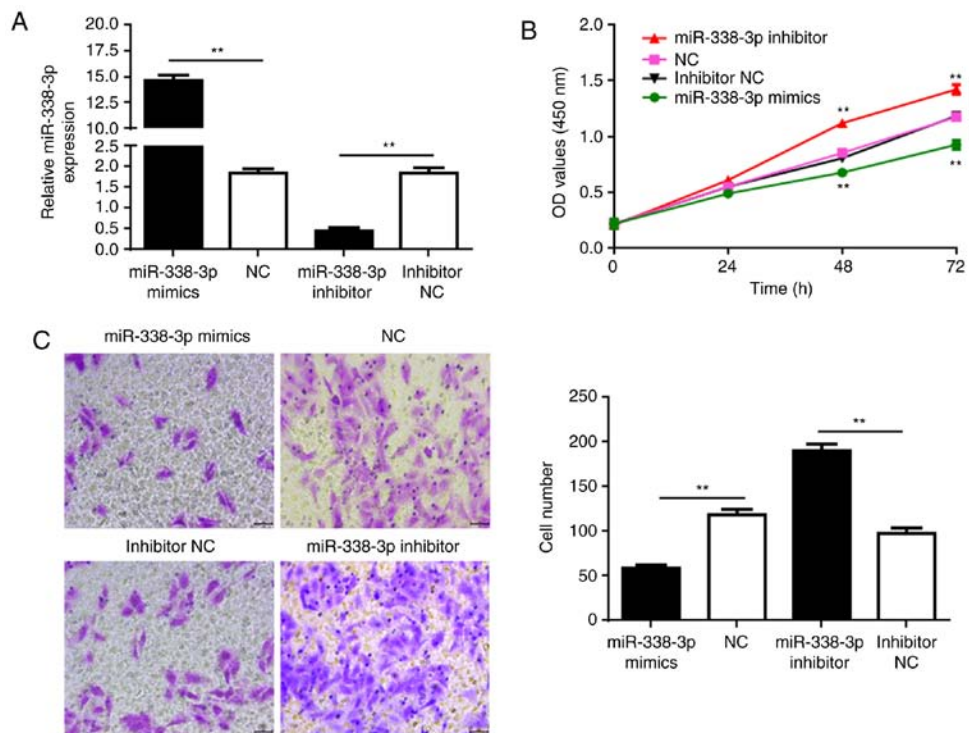


Figure 2. miR-338-3p inhibits the proliferation and migration of cultured SUP-T1 cells. (A) miR-338-3p levels in SUP-T1 cells transfected with miR-338-3p mimic, NC, miR-338-3p inhibitor or inhibitor NC. (B) Proliferation of SUP-T1 cells transfected with the aforementioned RNAs. (C) Migration of SUP-T1 cells transfected with the RNAs. Left, crystal violet-stained cells that migrated during the Transwell assay. Right, quantification of cell migration. Scale bar, 100 μ m. **P<0.01. miR-338-3p, microRNA-338-3p; NC, negative control; OD, optical density.

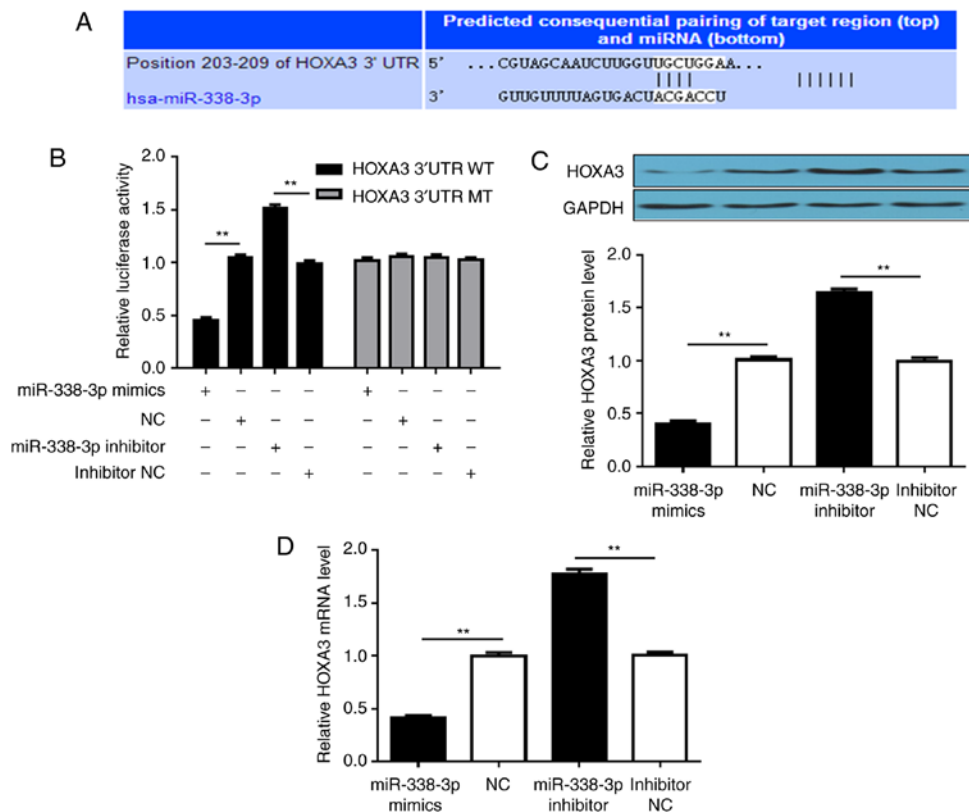


Figure 3. miR-338-3p targets the 3'-UTR of HOXA3 mRNA. (A) Predicted binding site of miR-338-3p in the 3'-UTR of HOXA3 mRNA. The paired sequence is highlighted by vertical lines. (B) Luciferase reporter assays investigating the effect of miR-338-3p on the 3'-UTR of HOXA3 mRNA. SUP-T1 cells were transfected with reporter vectors containing the WT or MT 3'-UTR of HOXA3, and were also transfected with miR-338-3p mimic, NC, miR-338-3p inhibitor or inhibitor NC. (C) Western blot analysis of HOXA3 protein expression in SUP-T1 cells transfected with the aforementioned RNAs. (D) Reverse transcription-quantitative PCR analysis of HOXA3 mRNA levels in SUP-T1 cells transfected with the aforementioned RNAs. **P<0.01. miR-338-3p, microRNA-338-3p; 3'-UTR, 3'-untranslated region; HOXA3, homeobox A3; NC, negative control; MT, mutant; WT, wild-type.

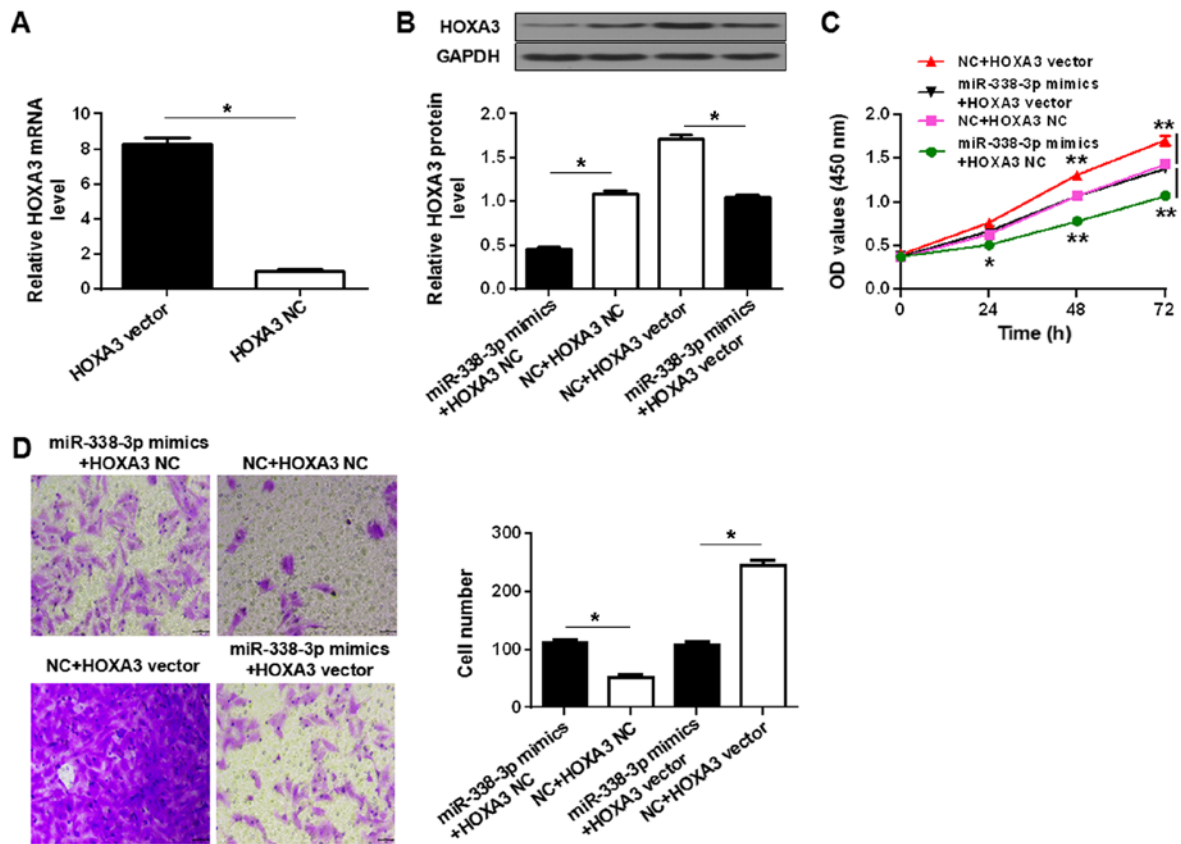


Figure 4. miR-338-3p-dependent downregulation of HOXA3 is required for the suppression of T-LBL malignancy. (A) Reverse transcription-quantitative polymerase chain reaction analysis of HOXA3 expression in SUP-T1 cells transfected with HOXA3 vector or NC. (B) Western blot analysis of HOXA3 protein levels in SUP-T1 cells co-transfected with HOXA3 vector or HOXA3 NC, and miR-338-3p mimics or NC. (C) Proliferation of SUP-T1 cells co-transfected with the aforementioned vectors and RNAs. (D) Migration of SUP-T1 cells transfected with the aforementioned vectors and miRNAs. Left, crystal violet-stained cells that migrated during the Transwell assay. Right, quantification of cell migration. Scale bar, 40 μ m. * P <0.05, ** P <0.01. miR-338-3p, microRNA-338-3p; HOXA3, homeobox A3; NC, negative control; HOXA3 NC, empty vector; OD, optical density.

miR-338-3p suppresses SUP-T1 cell proliferation and migration via the inhibition of HOXA3 protein expression. To determine whether the regulation of HOXA3 expression was involved in the tumor-suppressive role of miR-338-3p, the effects of miR-338-3p upregulation in the presence or absence of HOXA3 overexpression were determined. Transfection of SUP-T1 cells with HOXA3 vector significantly upregulated the expression of HOXA3 mRNA and protein compared with HOXA3 NC, whereas transfection with miR-338-3p mimics significantly reduced the expression of HOXA3 protein compared with the NC (Fig. 4A and B). Co-transfection of HOXA3 vector and miR-338-3p mimics did not significantly alter the protein level compared with co-transfection with the respective controls (Fig. 4B). Upregulation of HOXA3 significantly increased the proliferation and migration of the SUP-T1 cells compared with HOXA3 NC, and rescued proliferation and migration in miR-338-3p mimics-transfected cells (Fig. 4C and D). The results suggested that miR-338-3p suppressed T-LBL by inhibiting HOXA3 protein expression.

Discussion

T-LBL is an aggressive disease caused by the malignant transformation of immature progenitors primed towards T-cell development. At present, chemotherapy remains the main treatment option (1). This often includes intensive remission

induction chemotherapy, CNS prophylaxis, consolidation chemotherapy and subsequent maintenance therapy for 12-18 months (19); however, relapse is common and overall survival is poor (1). The present study observed that the expression profile of miR-338-3p may be important for the suppression of T-LBL. This miRNA was shown to directly target the 3'-UTR of HOXA3 mRNA to inhibit T-LBL cell proliferation and migration. The results provide insight for further investigation into signaling networks associated with miR-338-3p, and may aid the development of novel therapeutic options to reduce the incidence of relapse.

Studies on a variety of cancer types have reported the tumor-suppressive effects of miR3383p; therefore, there has been increasing interest in utilizing miR-338-3p to treat different solid tumors, including gastric cancer, hepatocellular carcinoma and malignant melanoma (20-22). The present study has associated miR-338-3p expression with the suppression of T-LBL for the first time, to the best of our knowledge. Notably, its target mRNA is encoded by the homeobox gene HOXA3. Numerous members of this gene family encode transcriptional factors that are mainly involved in embryonic development and hematopoietic stem cell function (23,24). Normal expression of HOXA3 in the developing embryo is required for the proper formation of the thymus, thyroid and parathyroid organs (23,24). HOXA3 overexpression, which can activate oncogenic signaling pathways, has been reported

to be involved in cancer biology (25). Further investigation into the mechanism of action of HOXA3 in T-LBL may aid the identification of molecular mechanisms involved in the development of the disease.

The molecular mechanisms of action of miRNAs on mRNAs have been extensively studied; however, the functional consequences remain unclear. It was initially hypothesized that miRNAs may inhibit the translation of target mRNAs without significantly affecting their levels in animal cells (26,27); however, it was subsequently proposed that the immediate outcome of miRNA-target mRNA interactions is translation inhibition, but that mRNA degradation can follow (28,29). The present study observed that HOXA3 protein and mRNA were downregulated by miR-338-3p in SUP-T1 cells, potentially supporting the idea that miRNAs induce target mRNA degradation; however, the possibility that miR-338-3p regulates other cellular factors that ultimately affect the transcription of the HOXA3 mRNA cannot be ruled out. A time-course analysis of the effects of miR-338-3p may help to further demonstrate the mechanisms underlying the actions of miR-338-3p.

Small animal models of human diseases, particularly rare diseases such as T-cell lymphoma/leukemia, are useful tools for investigating the molecular mechanisms underlying pathogenesis and evaluating novel therapeutic approaches. T-cell lymphoma has been modeled in various types of genetically modified mice, and although important insight has been obtained from these models, the limitations cannot be ignored (30), as no single animal model can capture all aspects of a human disease. Studies revealing novel molecular details regarding the development of T-LBL may improve rodent models, and thus aid research and development for the next generation of therapies.

Acknowledgements

Not applicable.

Funding

No funding was received.

Availability of data and materials

The datasets used and/or analyzed during the current study are available from the corresponding author on reasonable request.

Authors' contributions

XW designed the experiments. LW and MS performed the experiments and collected data. XW analyzed the data and drafted this manuscript. All authors approved this manuscript.

Ethics approval and consent to participate

Informed consent was obtained from all participants. The use of human samples was approved by the Human Ethics Committee/Institutional Review Board of the Affiliated Yantai Yuhuangding Hospital of Qingdao University.

Patient consent for publication

Not applicable.

Competing interests

The authors declare that they have no competing interests.

References

1. Uckun FM, Gaynon PS, SENSEL MG, Nachman J, Trigg ME, Steinherz PG, Hutchinson R, Bostrom BC, Sather HN and Reaman GH: Clinical features and treatment outcome of childhood T-lineage acute lymphoblastic leukemia according to the apparent maturational stage of T-lineage leukemic blasts: A children's cancer group study. *J Clin Oncol* 15: 2214-2221, 1997.
2. Lepretre S, Graux C, Touzart A, Macintyre E and Boissel N: Adult T-type lymphoblastic lymphoma: Treatment advances and prognostic indicators. *Exp Hematol* 51: 7-16, 2017.
3. Portell CA and Sweetenham JW: Adult lymphoblastic lymphoma. *Cancer J* 18: 432-438, 2012.
4. Lee WJ, Moon HR, Won C, Chang SE, Choi JH, Moon KC and Lee MW: Precursor B- or T-lymphoblastic lymphoma presenting with cutaneous involvement: A series of 13 cases including 7 cases of cutaneous T-lymphoblastic lymphoma. *J Am Acad Dermatol* 70: 318-325, 2014.
5. Aifantis I, Raetz E and Buonamici S: Molecular pathogenesis of T-cell leukaemia and lymphoma. *Nat Rev Immunol* 8: 380-390, 2008.
6. Graux C, Cools J, Michaux L, Vandenberghe P and Hagemeijer A: Cytogenetics and molecular genetics of T-cell acute lymphoblastic leukemia: From thymocyte to lymphoblast. *Leukemia* 20: 1496-1510, 2006.
7. Palomero T, Lim WK, Odom DT, Sulis ML, Real PJ, Margolin A, Barnes KC, O'Neil J, Neuberg D, Weng AP, *et al*: NOTCH1 directly regulates c-MYC and activates a feed-forward-loop transcriptional network promoting leukemic cell growth. *Proc Natl Acad Sci USA* 103: 18261-18266, 2006.
8. Weng AP, Millholland JM, Yashiro-Ohtani Y, Arcangeli ML, Lau A, Wai C, Del Bianco C, Rodriguez CG, Sai H, Tobias J, *et al*: c-Myc is an important direct target of Notch1 in T-cell acute lymphoblastic leukemia/lymphoma. *Genes Dev* 20: 2096-2109, 2006.
9. Vilimas T, Mascarenhas J, Palomero T, Mandal M, Buonamici S, Meng F, Thompson B, Spaulding C, Macaroun S, Alegre ML, *et al*: Targeting the NF-kappaB signaling pathway in Notch1-induced T-cell leukemia. *Nat Med* 13: 70-77, 2007.
10. Palomero T, Sulis ML, Cortina M, Real PJ, Barnes K, Ciofani M, Caparros E, Buteau J, Brown K, Perkins SL, *et al*: Mutational loss of PTEN induces resistance to NOTCH1 inhibition in T-cell leukemia. *Nat Med* 13: 1203-1210, 2007.
11. O'Neil J, Grim J, Strack P, Rao S, Tibbitts D, Winter C, Hardwick J, Welcker J, Meijerink JP, Pieters R, *et al*: FBW7 mutations in leukemic cells mediate NOTCH pathway activation and resistance to gamma-secretase inhibitors. *J Exp Med* 204: 1813-1824, 2007.
12. Weng AP, Ferrando AA, Lee W, Morris JP IV, Silverman LB, Sanchez-Irizarry C, Blacklow SC, Look AT and Aster JC: Activating mutations of NOTCH1 in human T cell acute lymphoblastic leukemia. *Science* 306: 269-271, 2004.
13. Ye F: MicroRNA expression and activity in T-cell acute lymphoblastic leukemia. *Oncotarget* 9: 5445-5458, 2018.
14. Wallaert A, Van Loocke W, Hernandez L, Taghon T, Speleman F and Van Vlierberghe P: Comprehensive miRNA expression profiling in human T-cell acute lymphoblastic leukemia by small RNA-sequencing. *Sci Rep* 7: 7901, 2017.
15. Saba R, Goodman CD, Huzarewich RL, Robertson C and Booth SA: A miRNA signature of prion induced neurodegeneration. *PLoS One* 3: e3652, 2008.
16. Li Y, Chen P, Zu L, Liu B, Wang M and Zhou Q: MicroRNA-338-3p suppresses metastasis of lung cancer cells by targeting the EMT regulator Sox4. *Am J Cancer Res* 6: 127-140, 2016.
17. Lister TA, Crowther D, Sutcliffe SB, Glatstein E, Canellios GP, Young RC, Rosenberg SA, Coltman CA and Tubiana M: Report of a committee convened to discuss the evaluation and staging of patients with Hodgkin's disease: Cotswolds meeting. *J Clin Oncol* 7: 1630-1636, 1989.

18. Livak KJ and Schmittgen TD: Analysis of relative gene expression data using real-time quantitative PCR and the 2- $\Delta\Delta$ CT method. *Methods* 25: 402-408, 2001.
19. Sweetenham JW: Treatment of lymphoblastic lymphoma in adults. *Oncology (Williston Park)* 23: 1015-1020, 2009.
20. Guo B, Liu L, Yao J, Ma R, Chang D, Li Z, Song T and Huang C: miR-338-3p suppresses gastric cancer progression through a PTEN-AKT axis by targeting P-REX2a. *Mol Cancer Res* 12: 313-321, 2014.
21. Huang XH, Wang Q, Chen JS, Fu XH, Chen XL, Chen LZ, Li W, Bi J, Zhang LJ, Fu Q, *et al*: Bead-based microarray analysis of microRNA expression in hepatocellular carcinoma: miR-338 is downregulated. *Hepatol Res* 39: 786-794, 2009.
22. Caramuta S, Egyhazi S, Rodolfo M, Witten D, Hansson J, Larsson C and Lui WO: MicroRNA expression profiles associated with mutational status and survival in malignant melanoma. *J Invest Dermatol* 130: 2062-2070, 2010.
23. Chojnowski JL, Masuda K, Trau HA, Thomas K, Capecchi M and Manley NR: Multiple roles for HOXA3 in regulating thymus and parathyroid differentiation and morphogenesis in mouse. *Development* 141: 3697-3708, 2014.
24. Manley NR and Capecchi MR: The role of Hoxa-3 in mouse thymus and thyroid development. *Development* 121: 1989-2003, 1995.
25. Zhang X, Liu G, Ding L, Jiang T, Shao S, Gao Y and Lu Y: HOXA3 promotes tumor growth of human colon cancer through activating EGFR/Ras/Raf/MEK/ERK signaling pathway. *J Cell Biochem* 119: 2864-2874, 2018.
26. Lee RC, Feinbaum RL and Ambros V: The *C. elegans* heterochronic gene *lin-4* encodes small RNAs with antisense complementarity to *lin-14*. *Cell* 75: 843-854, 1993.
27. Wightman B, Ha I and Ruvkun G: Posttranscriptional regulation of the heterochronic gene *lin-14* by *lin-4* mediates temporal pattern formation in *C. elegans*. *Cell* 75: 855-862, 1993.
28. Guo H, Ingolia NT, Weissman JS and Bartel DP: Mammalian microRNAs predominantly act to decrease target mRNA levels. *Nature* 466: 835-840, 2010.
29. Bazzini AA, Lee MT and Giraldez AJ: Ribosome profiling shows that miR-430 reduces translation before causing mRNA decay in zebrafish. *Science* 336: 233-237, 2012.
30. Kohnken R, Porcu P and Mishra A: Overview of the use of murine models in leukemia and lymphoma research. *Front Oncol* 7: 22, 2017.



This work is licensed under a Creative Commons Attribution-NonCommercial-NoDerivatives 4.0 International (CC BY-NC-ND 4.0) License.